

Barium nuclear magnetic resonance spectroscopic study of $\text{YBa}_2\text{Cu}_3\text{O}_7$

Jay Shore, Shengtian Yang, Jürgen Haase, Dwight Schwartz, and Eric Oldfield

*School of Chemical Sciences, University of Illinois at Urbana-Champaign, 505 South Mathews Avenue, Urbana, Illinois 61801
and Materials Research Laboratory, University of Illinois at Urbana-Champaign,
104 South Goodwin Avenue, Urbana, Illinois 61801*

(Received 25 November 1991)

We have measured the ^{135}Ba nuclear magnetic resonance (NMR) line shape and the ^{137}Ba nuclear quadrupole resonance (NQR) of a powder sample of $\text{YBa}_2\text{Cu}_3\text{O}_7$, at 300 K, as well as the temperature and field dependences of the $^{135,137}\text{Ba}$ NMR line shapes and spin-lattice relaxation rates of magnetically aligned ($c\parallel H_0$) samples, in the normal and superconducting states. From the NQR and the field and isotopic dependences of the NMR line shapes of magnetically aligned samples at 300 K, we conclude that the magnetic shift is small ($0.0\pm 0.12\%$), and that the principal components of the electric-field gradient tensor are $\pm(8.3, -0.2, -8.1)\times 10^{21}\text{ V m}^{-2}$, with the largest component coincident with the crystallographic c axis. In the superconducting state, the resonances broaden and are shifted to lower frequency. The spin-lattice relaxation behavior is not Korringa-like above T_c , and may be influenced by spin fluctuations in the CuO_2 plane.

INTRODUCTION

Nuclear magnetic resonance (NMR) spectroscopy is proving to be an important technique with which to probe the electronic and magnetic structures of the oxide superconductors, with many workers focusing on the $\text{YBa}_2\text{Cu}_3\text{O}_{7-x}$ system.¹⁻¹⁴ There have been detailed reports regarding the ^{17}O , $^{63,65}\text{Cu}$, and ^{89}Y NMR of $\text{YBa}_2\text{Cu}_3\text{O}_{7-x}$, but only recently has the barium site been probed using magnetic resonance techniques.^{15,16} In this paper, we report variable temperature measurements of the line shapes and longitudinal relaxation of $^{135,137}\text{Ba}$ NMR in $\text{YBa}_2\text{Cu}_3\text{O}_7$, using both powder and magnetically aligned, isotopically labeled samples, as well as ^{137}Ba nuclear quadrupole resonance (NQR) results at 300 K. Our results provide accurate values for the individual elements of the electric-field gradient tensor, in good agreement with previous theoretical work and recent unpublished results by Yakubowskii, Egorov, and Lütgemeier,¹⁶ put some limits on the magnitude (and direction) of the Knight shift, and also suggest that the barium site may be affected by magnetic spin excitations.

EXPERIMENT

Isotopically labeled samples were prepared from CuO , Y_2O_3 , and isotopically labeled BaCO_3 , using standard ceramic techniques.¹⁷ The barium carbonate was prepared from $^{135}\text{Ba}(56.6\%)(\text{NO}_3)_2$ or $^{137}\text{Ba}(89.6\%)(\text{NO}_3)_2$ (Oak Ridge National Laboratory, Oak Ridge, TN). Powder x-ray-diffraction data (Rigaku D/max diffractometer) indicated that all samples were single phase and fully oxygenated, and were in accord with literature diffraction patterns.^{18,19} Measurements of the magnetic susceptibility at low field (≤ 25 G) were made using a superconducting quantum interference magnetometer (Quantum Design, San Diego, CA), and the results showed that all samples were bulk superconductors, hav-

ing superconducting transition temperature (T_c) onsets of 92 K.

$^{135,137}\text{Ba}$ NMR spectra were obtained at 8.45 and 11.7 T with a spin-echo technique,²⁰ using two "homebuilt" spectrometers, which have been described previously.² Magnetically aligned samples were prepared from powders which had been passed through a stainless steel (No. 400 or No. 325) mesh, then mixed with epoxy resin (Duro, Cleveland, OH) and cured at either 8.45 or 11.7 T. Variable temperature measurements were made at 8.45 T with a continuous flow cryostat (model CF1200, Oxford Instruments, Osney Mead, United Kingdom). Frequency shifts are reported relative to an external 0.1 molar BaCl_2 standard solution, with high-frequency, low-field, paramagnetic or deshielded values being designated as positive (International Union of Pure and Applied Chemistry, IUPAC, δ scale). The absolute resonance frequencies of ^{135}Ba and ^{137}Ba are $^{135}\Xi=9.934$ and $^{137}\Xi=11.112$ (corresponding to the Ba resonance frequencies in 1 molar BaCl_2 in a field at which H in tetramethylsilane resonates at 100.000 000 MHz). Relaxation measurements were made using a three-pulse inversion-recovery sequence on magnetically aligned samples ($H_0\parallel c$). Pure NQR results were obtained using the 11.7 T NMR spectrometer console and a spin-echo pulse technique.

In Fig. 1, we show a plot of the ^{135}Ba NMR spin-echo intensity, as a function of frequency, for a powder sample of $\text{Y}^{135}\text{Ba}_2\text{Cu}_3\text{O}_7$, at 11.7 T, together with two computer-simulated line shapes. The data points were collected, typically in 100-kHz intervals, over a range of almost 7 MHz, and each point represents the integrated intensity of the Fourier-transformed spectrum from 30 000 spin echoes. The average linewidth of each spectrum was about 70 kHz, approximately the bandwidth of the radio frequency pulse excitation. A background subtraction was made using a similarly prepared, natural abundance sample, measured under identical conditions. A small correction was also made for the frequency dependence of the sensitivity of our NMR spectrometer. A similar mea-

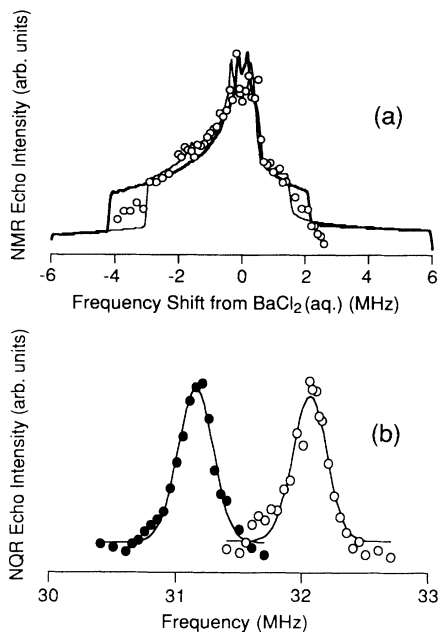


FIG. 1. Ba NMR and NQR spectra and simulations of powder samples of $Y^{135}\text{Ba}_2\text{Cu}_3\text{O}_7$ and $Y^{137}\text{Ba}_2\text{Cu}_3\text{O}_7$, respectively. (a) 11.7 T ^{135}Ba spin-echo spectrum of $Y^{135}\text{Ba}_2\text{Cu}_3\text{O}_7$ at 300 K, together with two computer simulations. Simulation parameters: bold line, $\nu_Q = 18.27$ MHz, $\eta = 0.94$; narrow line, $\nu_Q = 16$ MHz, $\eta = 0.8$. Spectral signal-to-noise ratios, magnetoacoustic ringing, and possible orientational ordering precluded accurate edge definition in the random powder. (b) NQR spectra of ^{63}Cu (●) and ^{137}Ba (○) in $Y^{137}\text{Ba}_2\text{Cu}_3\text{O}_7$, at 300 K, fit to Gaussians. The intensities of the two spectra are not to scale. Samples of $Y^{135}\text{Ba}_2\text{Cu}_3\text{O}_7$ have negligible NQR signal intensity at 32 MHz (data not shown).

surement of the ^{137}Ba NMR powder pattern would have required a much larger frequency range, due to the larger quadrupole moment ($^{135}Q/^{137}Q = 0.649$),^{21–25} and was not carried out.

Due to the very large size of the quadrupole interaction, a second-order calculation was expected to be inadequate. Hence, numerical diagonalization of the total Hamiltonian ($\mathcal{H}_{\text{Zeeman}} + \mathcal{H}_{\text{quadrupole}}$) was performed, with intensities from the central and the satellite transitions being included. The dependence of the amplitude of each transition on orientation was neglected. The powder average was performed by using an algorithm suggested by Alderman, Solum, and Grant.²⁶ Finally, the pattern was convoluted with a Gaussian line of 70 kHz width (the experimental bandwidth). Unfortunately, due to spectral signal-to-noise ratio limitations (because of the ~ 7 MHz overall linewidth), we were unable to obtain a unique solution for the quadrupole frequency, ν_Q , and the asymmetry parameter of the electric-field gradient tensor, η . The two simulations shown are for $\nu_Q = 16$ MHz, $\eta = 0.80$; and $\nu_Q = 18.27$ MHz, $\eta = 0.94$. Lütgemeier kindly informed us of his pure NQR results, which were only consistent with the latter value. We show in Fig. 1(b) the ^{137}Ba (and ^{63}Cu) NQR results we have obtained from our sample, at 300 K, fit to Gaussians. (The relative intensities of

the two resonances cannot be compared due to the difference in experimental conditions necessitated by the difference in gyromagnetic ratios.) The pure NQR frequency, ν_{NQR} , is related to ν_Q (and the quadrupole coupling constant, e^2qQ/h), for $I = \frac{3}{2}$, as

$$\nu_{\text{NQR}} = \nu_Q \left(1 + \frac{\eta^2}{3} \right)^{1/2} = \frac{e^2qQ}{2h} \left(1 + \frac{\eta^2}{3} \right)^{1/2}. \quad (1)$$

From the results shown in Fig. 1, and using the ratio of quadrupole moments, we find that $^{137}\nu_{\text{NQR}} = 32.06$ MHz, $^{135}\nu_Q \approx 18$ MHz, $^{137}\nu_Q \approx 28$ MHz, and $\eta \approx 0.94$, at 300 K.

More accurate values of ν_Q and η can be obtained by using ^{135}Ba , ^{137}Ba -labeled magnetically aligned samples at two magnetic-field strengths. Due to the anisotropic magnetic susceptibility of $Y\text{Ba}_2\text{Cu}_3\text{O}_7$ in the normal state, crystallites align in a magnetic field (H_0) with $c \parallel H_0$.²⁷ This leads to relatively narrow line spectra, but small ordering effects in powder samples can make edge definition difficult, and could be important in Fig. 1(a).

In Fig. 2, we show a plot of $^{135,137}\text{Ba}$ NMR spin-echo intensity as a function of frequency, for magnetically aligned ($c \parallel H_0$) samples, at 8.45 and 11.7 T, together with computer-simulated line shapes. The data points were collected as previously described for the random powder sample, but in a smaller, variable frequency increment. The line shapes shown were calculated with the largest

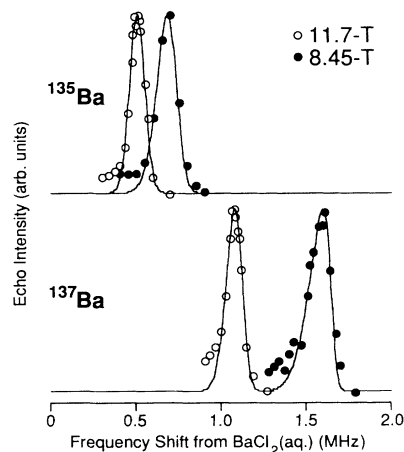


FIG. 2. Plots of $^{135,137}\text{Ba}$ NMR spin-echo intensity as a function of frequency offset for isotopically labeled, magnetically aligned ($c \parallel H_0$) samples of $Y\text{Ba}_2\text{Cu}_3\text{O}_7$, at 8.45 T (●) and 11.7 T (○), together with computer-simulated line shapes. The data points were collected in varying increments, and are the peak intensities at the carrier frequency for each individual offset spectrum. The line shapes were calculated by diagonalization of the total Hamiltonian, with V_{zz} coincident with the crystallographic c axis, using a 0.6° – 1.5° Gaussian distribution of crystallite orientations, an asymmetry parameter of 0.94, and quadrupole frequencies of 18.27 and 28.18 MHz for ^{135}Ba and ^{137}Ba , respectively. The absolute resonance frequency for ^{135}Ba was $^{135}\Xi = 9.934$ and for ^{137}Ba , $^{137}\Xi = 11.112$ (corresponding to the Ba resonance frequency in a field at which H in TMS resonates at 100.000000 MHz).

TABLE I. Electric-field gradient tensor elements of barium 135,137 in YBa₂Cu₃O₇.

		V_{aa} (10^{21} V m ⁻²)	V_{bb} (10^{21} V m ⁻²)	V_{cc} (10^{21} V m ⁻²)
Experiment	This report ^a	-8.1	-0.2	8.3
	Lütgemeier <i>et al.</i> ^b	-8.35	-0.35	8.70
Theory	Schwarz <i>et al.</i> ^c	-6.7	-0.6	7.3
	Yu <i>et al.</i> ^d	-5.65	-0.6	6.22

^aAt 300 K, the signs and V_{aa} and V_{bb} were assigned using the theoretical results of Refs. 28 and 32.

^bAt 4.2 K, Ref. 16.

^cReference 28.

^dReference 32.

component of the electric-field gradient tensor (V_{zz}) coincident with the crystallographic c axis. A standard deviation of the orientation of the crystallites of 0.6° – 1.5° , and a Gaussian line broadening of 40–60 kHz (depending on isotope and field), an asymmetry parameter of 0.94, and quadrupole frequencies of 18.27 and 28.18 MHz for ¹³⁵Ba and ¹³⁷Ba, respectively, were used in the simulations. The asymmetry parameter of 0.94 ± 0.02 was determined from theoretical fits of the oriented spectra, and by using the ν_{NQR} results of Fig. 1(b). The same procedure (including numerical diagonalization of the total Hamiltonian) as described above for the powder sample was used, except that we assumed that the crystallites had a Gaussian distribution of orientations relative to the static field, due to imperfect alignment in the epoxy resin. The two Euler angles, describing the relative position of the principal axis system of the electric-field gradient tensor with respect to the laboratory frame, were appropriately distributed. From the calculated line shapes, and using the following values of the quadrupole moments:^{21–25} $^{135}\text{Q} = 0.18(2) \times 10^{-24}$ cm², $^{137}\text{Q} = 0.28(3) \times 10^{-24}$ cm², we conclude that the electric-field gradient tensor for the barium site is $\pm(8.3, -0.2, -8.1) \times 10^{21}$ V m⁻², with V_{zz} coincident with the crystallographic c axis, at 300 K. The oriented spectra can also be adequately simulated using $^{135}\nu_{\text{Q}} = 16$ MHz and $\eta = 0.8$ [the same parameters as used for one of the simulations shown in Fig. 1(a), the narrow line], with V_{zz} perpendicular to the c axis. However, these parameters are inconsistent with the NQR results. The NQR and NMR measurements using the powder and magnetically aligned samples are in basically good agreement with the results of *ab initio* calculations made by Blaha and co-workers^{28–31} [$(7.3, -0.72, -6.46) \times 10^{21}$ V m⁻²] and Yu *et al.*³² [$(6.2, -0.6, -5.6) \times 10^{21}$ V m⁻²], as shown in Table I. The good overall agreement supports the correctness of their linear augmented-plane-wave approach for the barium site. In addition, our results are also (now) in good agreement with the unpublished results of Yakubowskii, Egorov, and Lütgemeier.¹⁶

Although the observed spectra are overwhelmingly dominated by quadrupolar effects, we can estimate the magnetic (chemical plus Knight) shift, for $c \parallel H_0$, using the spectra of Fig. 2, to be $0.00 \pm 0.12\%$ (00 ± 1200 ppm). The large uncertainty is due to the breadths of the resonances involved. We can compare this magnetic shift

with the chemical shifts of three diamagnetic model systems, Ba(NO₃)₂, -50 ppm; BaZrO₃, 293 ppm; BaTiO₃, 395 ppm (Ref. 33); and find them to be of comparable magnitude. Neglecting the temperature dependence of the quadrupole shift of the oriented sample spectra, our variable temperature results yield an upper limit of the Knight shift, since there is a 20 ± 10 kHz (25 ± 10 kHz) shift to lower frequency for ¹³⁵Ba (¹³⁷Ba) on cooling from 100 to 25 K. While demagnetization effects are sample dependent, the measurements of Barrett *et al.*⁵ provide an estimate of the difference between the magnetic field inside the sample (H_{int}) and the applied field (H_0) in the superconducting state. Barrett *et al.* found that at 4.2 K, H_{int} is 0.05% lower than H_0 for a magnetically aligned powder sample ($c \parallel H_0$). Thus, the change in the bulk susceptibility with the onset of superconductivity may account completely for the temperature dependence of the barium shift below T_c .

We have also measured spin-lattice relaxation rates in magnetically aligned samples as a function of temperature, and show in Fig. 3(a) the ¹³⁷Ba relaxation decays fit to single exponentials (at 8.45 T), for a range of tempera-

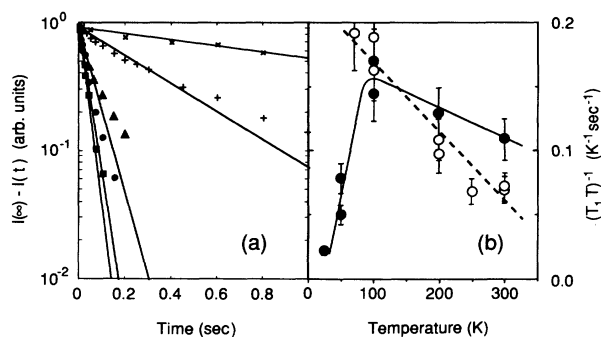


FIG. 3. 8.45 T spin-lattice relaxation results for ^{135,137}Ba in magnetically aligned, isotopically enriched samples of YBa₂Cu₃O₇. (a) ¹³⁷Ba decays at 300 K (■), 200 K (●), 100 K (▲), 50 K (+), and 25 K (×), fit to a single exponential. (b) ¹³⁵(1/ T_1T) and ¹³⁷(1/ T_1T) as a function of temperature, for magnetically aligned ($c \parallel H_0$), isotopically enriched samples of YBa₂Cu₃O₇: ¹³⁵Ba (○); ¹³⁷Ba (●). The lines are meant as guides to the eye; the dashed line corresponds to ¹³⁵Ba, the solid line to ¹³⁷Ba. The error bars are $\pm 15\%$.

tures, and $(1/T_1T)$ as a function of temperature for both isotopes, in Fig. 3(b). The lines in Fig. 3(b) are meant as guides to the eye. From the apparent difference in the functional forms of the decays, and the differences in the temperature dependences of the relaxation rates for the two isotopes, it appears that multiple relaxation mechanisms are involved. Due to difficulties associated with separating the effects of the different mechanisms, we have fitted the observed decays empirically to a single exponential time constant, T_1 . Fitting the decays to the expected multiple exponential expression (for magnetic relaxation) yields essentially the same temperature dependences. As can be seen in Fig. 3(b), the spin-lattice relaxation behavior of both Ba isotopes in $\text{YBa}_2\text{Cu}_3\text{O}_7$ is distinctly non-Korringa above T_c (i.e., T_1T is not constant). This result is somewhat surprising, given the Korringa behavior of the ^{89}Y and the CuO_2 planar ^{17}O sites. Thus it seems that, as with the CuO_2 planar copper, there is a constant (spin-fluctuation) contribution to the relaxation of both barium isotopes, due to a noncancellation of transferred hyperfine couplings.

On cooling below T_c (50, 25 K), we were able to deter-

mine the ^{137}Ba relaxation rates (the ^{135}Ba value were much longer), and again as shown in Fig. 3(b), it is clear that these rates decrease abruptly, as seen previously for other sites in $\text{YBa}_2\text{Cu}_3\text{O}_7$. We thus tentatively conclude that the barium site in $\text{YBa}_2\text{Cu}_3\text{O}_7$ more closely reflects the relaxation behavior of the plane, rather than chain, copper sites (or the plane, chain, or apical oxygen atoms)—based on the temperature dependences of the relaxation rates above T_c , and the sharp ^{137}Ba relaxation rate decrease below T_c .

ACKNOWLEDGMENTS

We are grateful to Lütgemeier for providing us with Ref. 16 prior to publication, and for several valuable conversations. We also thank Dean Thelen for his helpful comments. This work was supported in part by the Solid State Chemistry Program of the U.S. National Science Foundation (Grant No. DMR 88-14789) and in part by the Materials Research Laboratory (Grant No. 89-20538) (J.S., S.Y., and J.H.).

- ¹C. Coretsopoulos, H. C. Lee, E. Ramli, L. Reven, T. B. Rauchfuss, and E. Oldfield, *Phys. Rev. B* **39**, 781 (1989).
- ²E. Oldfield, C. Coretsopoulos, S. Yang, L. Reven, H. C. Lee, J. Shore, O. H. Han, E. Ramli, and D. S. Hinks, *Phys. Rev. B* **40**, 6832 (1989).
- ³L. Reven, J. Shore, S. Yang, T. Duncan, D. Schwartz, J. Chung, and E. Oldfield, *Phys. Rev. B* **43**, 10466 (1991).
- ⁴Y. Yoshinari, H. Yasuoka, Y. Ueda, K. Koga, and K. Kosuge, *J. Phys. Soc. Jpn.* **59**, 3698 (1990).
- ⁵S. E. Barrett, D. J. Durand, C. H. Pennington, C. P. Slichter, T. A. Friedmann, J. P. Rice, and D. M. Ginsberg, *Phys. Rev. B* **41**, 6283 (1990).
- ⁶H. Lütgemeier, *Hyperfine Interact.* **61**, 1051 (1990).
- ⁷H. Alloul, P. Mendels, G. Collin, and P. Monod, *Phys. Rev. Lett.* **61**, 746 (1988).
- ⁸J. T. Markert, T. W. Noh, S. E. Russek, and R. M. Cotts, *Solid State Commun.* **63**, 847 (1987).
- ⁹R. E. Walstedt and W. W. Warren, Jr., *Science* **248**, 1082 (1990).
- ¹⁰T. Imai, *J. Phys. Soc. Jpn.* **59**, 2508 (1990).
- ¹¹M. Takigawa, A. P. Reyes, P. C. Hammel, J. D. Thompson, R. H. Heffner, Z. Fisk, and K. C. Ott, *Phys. Rev. B* **43**, 247 (1991).
- ¹²S. E. Barrett, J. A. Martindale, D. J. Durand, C. H. Pennington, C. P. Slichter, T. A. Friedmann, J. P. Rice, and D. M. Ginsberg, *Phys. Rev. Lett.* **66**, 108 (1991).
- ¹³M. Takigawa, J. L. Smith, and W. L. Hults, *Phys. Rev. B* **44**, 7764 (1991).
- ¹⁴C. H. Pennington and C. P. Slichter, in *Physical Properties of High Temperature Superconductors*, edited by D. M. Ginsberg (World Scientific, Teaneck, NJ, 1990), Vol. II, and references cited within.
- ¹⁵H. Lütgemeier, V. Florentiev, and A. Yakubowskii, in *Electronic Properties of High- T_c Superconductors and Related Compounds*, edited by H. Kuzmany, M. Mehring, and J. Fink (Springer-Verlag, Berlin, 1990).
- ¹⁶A. Yakubowskii, A. Egorov, and H. Lütgemeier (unpublished).
- ¹⁷G. F. Holland and A. M. Stacy, *Acc. Chem. Res.* **21**, 8 (1988).
- ¹⁸*Chemistry of High-Temperature Superconductors*, edited by D. L. Nelson, M. S. Whittingham, and T. F. George (American Chemical Society, Washington, DC, 1987).
- ¹⁹H. Steinfink, J. S. Swinnea, Z. T. Sui, H. M. Hsu, and J. B. Goodenough, *J. Am. Chem. Soc.* **109**, 3348 (1987).
- ²⁰A. C. Kunwar, G. L. Turner, and E. Oldfield, *J. Magn. Res.* **69**, 124 (1986).
- ²¹S. Nakamura and H. Enokiya, *J. Phys. Soc. Jpn.* **18**, 183 (1963).
- ²²A. F. Volkov, *J. Magn. Res.* **11**, 73 (1973).
- ²³I.-J. Ma and G. zu Putlitz, *Z. Phys. A* **277**, 107 (1976).
- ²⁴H. Krüger, O. Lutz, and H. Oehler, *Phys. Lett.* **62A**, 131 (1977).
- ²⁵O. Lutz and H. Oehler, *Z. Phys. A* **288**, 11 (1978).
- ²⁶D. W. Alderman, M. S. Solum, and D. M. Grant, *J. Chem. Phys.* **84**, 3717 (1986).
- ²⁷D. E. Farrell, B. S. Chandrasekhar, M. R. DeGuire, M. M. Fang, V. G. Kogan, J. R. Clem, and D. K. Finnemore, *Phys. Rev. B* **36**, 4025 (1987).
- ²⁸K. Schwarz, C. Ambrosch-Draxl, and P. Blaha, *Phys. Rev. B* **42**, 2051 (1990).
- ²⁹C. Ambrosch-Draxl, P. Blaha, and K. Schwarz, *Hyperfine Interact.* **61**, 1117 (1990).
- ³⁰K. Schwarz, P. Blaha, and C. Ambrosch-Draxl, *Int. J. Quantum Chem.* **24**, 339 (1990).
- ³¹C. Ambrosch-Draxl, P. Blaha, and K. Schwarz, in *Electronic Properties of High- T_c Superconductors and Related Compounds* (Ref. 15), Vol. 99, p. 338.
- ³²J. Yu, A. J. Freeman, R. Podloucky, P. Herzig, and P. Weinberger, *Phys. Rev. B* **43**, 532 (1991).
- ³³C. E. Forbes, W. B. Hammond, N. E. Cipollini, and J. F. Lynch, *J. Chem. Soc., Chem. Commun.* **1987**, 433.